troponin T or other extended parts of the *Limulus* troponin complex might also contribute to the strand density. By localizing *Limulus* tropomyosin (and possibly parts of troponin), in both the 'off' and 'on' states, to positions on actin originally proposed in the seminal steric model[1-3] and again more recently on the basis of further modelling[14,15], we offer direct structural support for the hypothesis. Earlier reconstructions of thin filaments reconstituted from vertebrate proteins either failed to resolve tropomyosin from actin[16,17], or revealed it only in the 'on' state[4,18], perhaps because in the vertebrate 'off' state tropomyosin is disordered[18] (R. A. Milligan, personal communication).

It is striking that the position adopted by *Limulus* tropomyosin in the 'off' state coincides with a myosin contact site on actin thought to be involved in a stereospecific and strong actomyosin interaction[19]. Hence tropomyosin in the 'off' state may compete for myosin attachment to this site. Our results therefore are consistent with a steric mechanism in which tropomyosin in relaxed muscle could interfere with the transition from an initially weak to a strong myosin crossbridge association on actin (compare ref. 20), thereby inhibiting ATPase and crossbridge cycling. Such a mechanism is no doubt a general feature of troponin-regulated muscles. □

Received 25 November 1993; accepted 18 January 1994.

1. Huxley, H. E. *Cold Spring Harbor Symp. quant. Biol.* **37,** 361–376 (1972).
2. Haselgrove, J. C. *Cold Spring Harbor Symp. quant. Biol.* **37,** 225–234 (1972).
3. Parry, D. A. D. & Squire, J. M. *J. molec. Biol.* **75,** 33–55 (1973).
4. Milligan, R. A., Whittaker, M. & Safer, D. *Nature* **348,** 217–221 (1990).
5. Lehman, W., Regenstein, J. M. & Ransom, A. L. *Biochim. biophys. Acta* **434,** 215–222 (1976).
6. Lehman, W. *J. molec. Biol.* **154,** 385–391 (1982).
7. Lehman, W. *Nature* **255,** 424–426 (1975).
8. Lehman, W. & Szent-Györgyi, A. G. *J. gen. Physiol.* **59,** 375–387 (1975).
9. Regenstein, J. M. & Szent-Györgyi, A. G. *Biochemistry* **14,** 917–925 (1975).
10. Bullard, B. *et al. J. molec. Biol.* **204,** 621–637 (1988).
11. Vibert, P., Craig, R. & Lehman, W. *J. Cell Biol.* **123,** 313–321 (1993).
12. Cohen, C. *et al. Cold Spring Harbor Symp. quant. Biol.* **37,** 287–297 (1972).
13. Flicker, P. F., Phillips, G. N. & Cohen, C. J. *molec. Biol.* **162,** 495–501 (1982).
14. Holmes, K. C. & Kabsch, W. *Curr. Opin. Struct. Biol.* **1,** 270–280 (1991).
15. Squire, J. M., Al-Khayat, H. A. & Yagi, N. *J. chem. Soc. Farad. Trans.* **89,** 2717-2726 (1993).
16. Seymour, J. & O'Brien, E. J. *Nature* **283,** 680–682 (1980).
17. Toyoshima, C. & Wakabayashi, T. *J. Biochem. (Tokyo)* **97,** 245–263 (1985).
18. O'Brien, E. J., Couch, J., Johnson, G. R. P. & Morris, E. P. in *Actin: Structure and Function in Muscle and Non-Muscle Cells* (eds dosRemedios, C. G. & Barden, J. A.) 3–15 (Academic, North Ryde, NSW, Australia, 1983).
19. Rayment, I. *et al. Science* **261,** 58–65 (1993).
20. Chalovich, J. M., Chock, P. B. & Eisenberg, E. *J. biol. Chem.* **256,** 575–587 (1981).
21. Moody, C., Lehman, W. & Craig, R. *J. Muscle Res. Cell Motil.* **11,** 176–185 (1990).
22. DeRosier, D. J. & Moore, P. B. *J. molec. Biol.* **52,** 355–369 (1970).
23. Amos, L. A. & Klug, A. *J. molec. Biol.* **99,** 51–73 (1975).
24. Trachtenberg, S. & DeRosier, D. J. *J. molec. Biol.* **195,** 581–601 (1987).
25. Milligan, R. A. & Flicker, P. F. *J. Cell Biol.* **105,** 29–39 (1987).

ACKNOWLEDGEMENTS. We thank C. Cohen for discussion and encouragement, A. McGough, D. Morgan and C. Owen for discussion and help with computer programs, and M. Picard Craig for photography. This work was supported by grants from the NIH (W.L., R.C. and C.C.) and from the NSF (P.V. and C.C.).

# Calcium channel β-subunit binds to a conserved motif in the I–II cytoplasmic linker of the $\alpha_1$-subunit

**Marlon Pragnell*, Michel De Waard*, Yasuo Mori†, Tsutomu Tanabe‡, Terry P. Snutch§ & Kevin P. Campbell*‖**

* Howard Hughes Medical Institute, Department of Physiology and Biophysics and Program in Neuroscience, University of Iowa College of Medicine, 400 EMRB, Iowa City, Iowa 52242, USA
† Department of Medical Chemistry, Kyoto University, Kyoto 606, Japan
‡ Howard Hughes Medical Institute, Department of Cellular and Molecular Physiology, Yale University, New Haven, Connecticut 06536, USA
§ Biotechnology Laboratory and Departments of Zoology and Neuroscience, University of British Columbia, Vancouver, British Columbia V6T 1Z3, Canada

**THE β-subunit is an integral component of purified voltage-sensitive $Ca^{2+}$ channels[1-3]. Modulation of $Ca^{2+}$ channel activity by the β-subunit, which includes significant increases in transmembrane current and/or changes in kinetics, is observed on coexpression of six $\alpha_1$-subunit genes with four β-subunit genes in all $\alpha_1$–β combinations tested[4-12]. Recent reports suggest that this regulation is not due to targeting of the $\alpha_1$-subunit to the plasma membrane but is probably a result of a conformational change induced by the β-subunit[11,13]. Here we report that the β-subunit binds to the cytoplasmic linker between repeats I and II of the dihydropyridine-sensitive $\alpha_1$-subunits from skeletal ($\alpha_{1S}$) and cardiac muscles ($\alpha_{1C-a}$), and also with the more distantly related neuronal $\alpha_{1A}$ and ω-conotoxin GVIA-sensitive $\alpha_{1B}$-subunits. Sequence analysis of the β-subunit binding site identifies a conserved motif (QQ-E--L-GY--WI---E) positioned 24 amino acids from the IS6 transmembrane domain in each $\alpha_1$-subunit. Mutations within this motif reduce the stimulation of peak currents by the β-subunit and alter inactivation kinetics and voltage-dependence of activation. Conservation of the β-subunit binding motif in these functionally distinct calcium channels suggests a critical role for the I–II cytoplasmic linker of the $\alpha_1$-subunit in channel modulation by the β-subunit.**

An $^{35}$S-labelled *in vitro*-translated rat $\beta_{1b}$-subunit[14] protein probe (Fig. 1*a*) was used to demonstrate an interaction between the β- and $\alpha_{1S}$-subunits of the dihydropyridine receptor (DHPR) from skeletal muscle. A single prominent radioactive band corresponding to a relative molecular mass of 170,000 ($M_r$ 170K) was detected in purified DHPR[15] which colocalized with immunostained $\alpha_{1S}$-subunit (Fig. 1*b*). On prolonged exposure, β-subunit interaction with the DHPR $\alpha_{1S}$-subunit was also detected in triads and T-tubule membranes. Incubations with $^{35}$S-labelled sham *in vitro* translates showed no interaction (not shown). In addition, the *in vitro*-translated $\beta_{1a}$-subunit of DHPR and the $\beta_3$-subunit of the ω-conotoxin GVIA receptor (CgTxR)[3] identified the same 170K protein, suggesting a conserved site for $\alpha_1$-subunit interaction among β-subunits from different genes (not shown).

To identify the β-subunit interaction site on the $\alpha_{1S}$-subunit, we screened an epitope library of the rabbit DHPR $\alpha_{1S}$-subunit[16] with the $^{35}$S-labelled $\beta_{1b}$-subunit probe. Figure 2*a* shows an autoradiogram of a single purified positive clone amplified and probed with the translated $\beta_{1b}$-subunit. Similar results were obtained with a $\beta_3$-probe (not shown), whereas an overlay of this $\alpha_{1S}$-positive clone with a $^{35}$S-labelled $\alpha_{2b}$-probe showed no interaction (Fig. 2*a*). Seven positive plaques were purified to homogeneity and DNA sequencing showed that all clones were in the appropriate reading frame. The epitopes ranged in size from 50 to 67 amino acids and all shared a 45-amino-acid overlap that extends from amino acid 341 to 385 of the $\alpha_{1S}$-subunit. Analysis of the transmembrane topology of the $\alpha_{1S}$-subunit maps this β-subunit interaction site to the putative cytoplasmic linker between repeats I and II and is consistent with the predicted cytoplasmic location of the β-subunit[1,2] (Fig. 2*d*).

Because coexpression of β-subunits with various $\alpha_1$-subunits greatly enhances peak inward currents and alters kinetic and voltage-dependent properties[4-12], we addressed whether this interaction site is conserved in distantly related calcium channel $\alpha_1$-subunits. We constructed epitope libraries of the complemen-

‖ To whom correspondence should be addressed.

tary DNA encoding the rabbit cardiac dihydropyridine-sensitive $\alpha_{1C\text{-}a}$-subunit[5] and the rat neuronal $\omega$-conotoxin GVIA-sensitive $\alpha_{1B}$-subunit[17]. Although these subunits exhibit the characteristic transmembrane topology of voltage-sensitive calcium channels, they are encoded by different genes and share only 66 and 34% identity, respectively, with the DHPR $\alpha_{1S}$. Positive clones were again detected with $^{35}$S-labelled $\beta_{1b}$-subunit probe and found to map to the same location on the I–II cytoplasmic linker of each $\alpha_1$-subunit. The smallest of two overlapping clones from the $\alpha_{1C\text{-}a}$ λgt11 expression library encoded an 84-amino-acid epitope extending from amino acids 434 to 517 of this subunit. Similarly, the smallest of two epitopes cloned from a screen of the $\alpha_{1B}$ library yielded a 56-amino-acid domain representing amino acids 378 to 434. To extend these observations to the $\alpha_{1A}$-subunit, which shares 33% identity with DHPR $\alpha_{1S}$, we constructed a glutathione-*S*-transferase (GST) fusion protein expressing

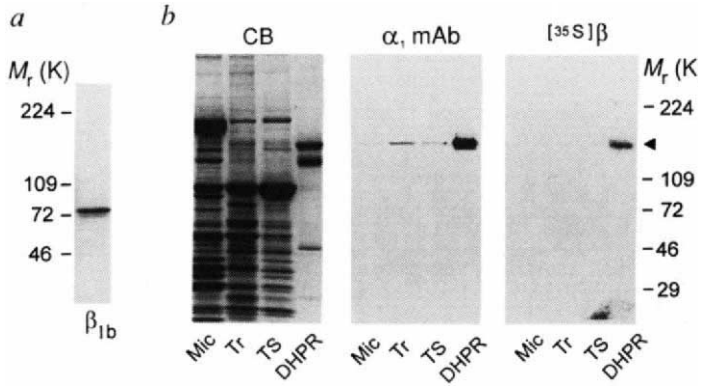


FIG. 1 $\beta$-Subunit interaction with the $\alpha_1$-subunit of the dihydropyridine-sensitive calcium channel from skeletal muscle. *a*, Autoradiogram of SDS–polyacrylamide gel of *in vitro*-translated $^{35}$S-labelled probe. The $\beta_{1b}$-subunit migrates differently from the $\beta_{1a}$ of DHPR because the primary structure of the $\beta_{1b}$ splice variant predicts it to have an $M_r$ 7.81K larger than $\beta_{1a}$[14]. *b*, CB, Coomassie blue-stained SDS–polyacrylamide gel of rabbit skeletal muscle crude membranes (Mic), triads (Tr), T-tubule system (TS) and purified dihydropyridine receptor (DHPR). $\alpha_1$ mAb, Corresponding immunoblot stained with a mix of monoclonal antibodies (mAbs IIF7, IIC12 and IIID5; ref. 15) to $\alpha_{1S}$ of DHPR. [$^{35}$S]$\beta$, Autoradiogram of an identical nitrocellulose transfer incubated with *in vitro*-translated [$^{35}$S]$\beta_{1b}$ probe. Arrowhead indicates the 170K protein, $\alpha_{1S}$.
METHODS. The [$^{35}$S]$\beta_{1b}$-subunit[14] probe was synthesized by coupled *in vitro* transcription and translation in the TNT system (Promega). To enhance probe yield, a 50-nucleotide alfalfa mosaic viral consensus initiation site was engineered into the cDNA. Translation was in the presence of a cocktail containing protease inhibitors pepstatin A, chymostatin, aprotinin, antipain and leupeptin (Boehringer Mannheim) at 0.1 μg ml$^{-1}$ and calf liver tRNA (Sigma) at 40 μg ml$^{-1}$ to minimize proteolysis and reduce background translation. Rabbit skeletal muscle crude membranes, triads, T-tubule system and purified dihydropyridine receptor[15] were electrophoretically separated on 3–12% SDS polyacrylamide gels in the presence of 1% 2-mercaptoethanol and transferred to nitrocellulose. These blots were blocked with 5% non-fat dry milk in 150 mM NaCl, 50 mM sodium phosphate (PBS), followed by an overlay buffer of 5% bovine serum albumin (BSA) and 0.5% non-fat dry milk in PBS. The translation reaction was added at 1 μl ml$^{-1}$ of overlay buffer and incubated with gentle mixing for 12 h at 4 °C. The transfers were washed 1 h with 5% BSA in PBS at room temperature, air-dried and exposed to film (X-OMAT AR, Kodak).

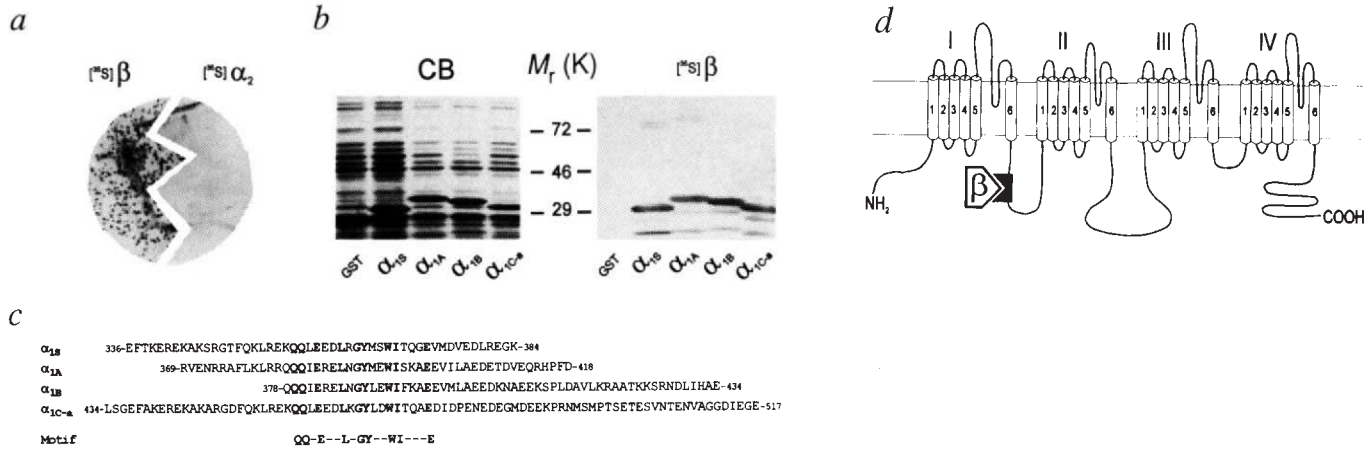


FIG. 2 Identification of the $\beta$-subunit interaction site on the $\alpha_1$-subunit by epitope cloning. *a*, Autoradiogram of an amplified single positive plaque isolated by screening a skeletal muscle DHPR $\alpha_{1S}$ subunit epitope library with an *in vitro*-translated [$^{35}$S]$\beta_{1b}$ subunit probe. The nitrocellulose lift was cut and each half was incubated with either the [$^{35}$S]$\beta_{1b}$ subunit or a [$^{35}$S]$\alpha_{2b}$ subunit probe. *b*, Coomassie blue-stained SDS–polyacrylamide gel of glutathione-S-transferase (GST) control and $\alpha_{1S}$, $\alpha_{1A}$, $\alpha_{1B}$ and $\alpha_{1C\text{-}a}$ epitopes expressed as GST fusion proteins in total *E. coli* lysate (left), and autoradiogram of corresponding overlay with [$^{35}$S]$\beta_{1b}$ subunit on these nitrocellulose-immobilized fusion proteins (right). *c*, Alignment of amino-acid sequences of these fusion protein epitopes identifying a conserved $\alpha_1$–$\beta$ subunit interaction motif. The first and last amino acids of each epitope are numbered according to their location in the primary structure, as deduced from the full-length cDNA. *d*, Schematic showing the $\beta$-subunit interaction site on the I–II cytoplasmic linker of the $\alpha_1$-subunit.
METHODS. $\alpha_1$-Subunit epitope libraries in the λgt11 vector were made by digesting the $\alpha_1$-subunit cDNA in a plasmid vector with DNAse I in the presence of 10 mM $MnCl_2$. Following the addition of *Eco*RI linkers, the randomly digested fragments were size-selected to <500 bp in Nusieve agarose gel (FMC Bioproducts). These fragments were then purified, digested with *Eco*RI and ligated into λgt11. The $\beta_{1b}$-subunit probe was used to screen $2 \times 10^4$ clones of each $\alpha_1$-subunit epitope library. Inserts were amplified from pure phage positives by polymerase chain reaction (PCR) using primers directed to λgt11 phage arms. These were directly subcloned into a T-vector[23] (made from Bluescript SK- plasmid) for sequencing, or digested with *Eco*RI and ligated into the pGEX1 vector for GST fusion protein production. A fusion protein epitope of the $\alpha_{1A}$ subunit was constructed by amplifying base pairs 1,387–1,553 with the following primers: 5′-AGGGAATTCAAAGGGATGTCTCTG-3′ and 5′-AAGGATCCGAGCGGGTGGAGAAC-3′. This PCR product was then digested with *Bam*HI and *Eco*RI and subcloned into the pGEX2T vector. All inserts were sequenced in both directions by the dideoxy chain termination method using Sequenase II (US Biochemicals). Each recombinant pGEX molecule was introduced into *E. coli* DH5α cells. Overnight cultures of the pGEX-epitope constructs were diluted 1:10, incubated for 1 h and induced for 2 h with 1 mM isopropyl-β-D-thiogalactopyranoside. 75 μl of each culture was dissolved in SDS sample buffer and proteins separated electrophoretically on 3–12% SDS–polyacrylamide gels and transferred to nitrocellulose. Overlays were done as described in the legend to Fig. 1 in 5% BSA and 0.5% non-fat dry milk in PBS. Peptide sequence homology searches were done at the National Center for Biotechnology Information using the BLAST[18] network service.

amino acids 369 to 418 of the rabbit neuronal $\alpha_{1A}$-subunit[12], which spans the region common to all cloned epitopes. As shown in Fig. 2*b*, the $\beta_{1b}$-subunit binds to the epitopes in all four $\alpha_1$-subunits when expressed as GST fusion proteins. All epitopes mapped to the I–II cytoplasmic linker, although a comparison of this linker sequence among the four $\alpha_1$-subunits shows only 19% overall identity.

Sequence comparison of the epitopes (Fig. 2*c*) suggests the presence of an interaction motif on each $\alpha_1$-subunit that can be minimally described by QQ-E--L-GY--WI---E. A BLAST[18] search with this motif identified sequence records representing all voltage-sensitive calcium channel $\alpha_1$-subunits so far reported. Although the lengths of the cytoplasmic linkers separating repeats I and II among these four $\alpha_1$-subunits vary in size from 99 to 129 amino acids, the conserved motif is always positioned 24 amino acids downstream from the S6 transmembrane element of repeat I. Splice variations in the I–II cytoplasmic linker encoded by the $\alpha_{1C}$ gene have been reported which are close to the motif and hence may be important in differential $\beta$-subunit regulation of these channels. These include a 33-amino-acid exon that replaces the IS6 transmembrane segment and a 25-amino-acid insertion positioned 19 residues downstream of the motif in the $\alpha_{1C}$ cloned from lung[19]. Three additional splice variations of this region in $\alpha_{1C}$ have been reported at a location immediately downstream of the latter insertion[20].

To perturb the $\beta$-subunit binding in the protein overlay assay and thereby identify candidate residues that contribute to the structural integrity of the motif, we made the following non-conservative mutations in the GST fusion protein (FP) epitope of the $\alpha_{1A}$-subunit: glutamate at position 4 of the motif to serine ($E386S_{FP}$), leucine at position 7 to histidine ($L389H_{FP}$), tyrosine at position 10 to serine ($Y392S_{FP}$) or glutamate at position 18 to alanine ($E400A_{FP}$). The ability of the mutants to interact with

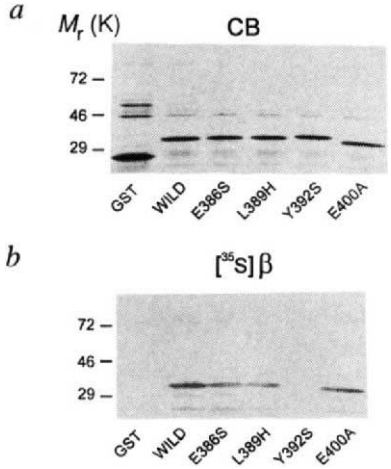


FIG. 3 Mutation of the motif in the $\alpha_{1A}$ epitope perturbs the $\beta$-subunit interaction in the overlay assay. *a*, Coomassie blue-stained SDS–polyacrylamide gel of GST, $\alpha_{1A}$ epitope (WILD) and mutants (E386S, L389H, Y392S and E400A) expressed as GST fusion proteins in total *E. coli* lysate, and *b*, autoradiogram of corresponding overlay with [$^{35}$S]$\beta_{1b}$-subunit probe on these nitrocellulose-immobilized GST fusion proteins. METHODS. Site-directed mutageneis was performed on the fusion protein containing the $\alpha_{1A}$ epitope using the Transformer site-directed mutagenesis system (Clontech). This method works by simultaneously annealing two oligonucleotide primers to one strand of a denatured double-stranded plasmid. One primer introduces the desired mutation and the second mutates a restriction site unique to the plasmid for the purpose of selection. To generate fusion protein mutants the following mutagenic primers were used: 5′-GCGGCAGCAGCAGATATCACG-CGAGCTCAACGGG-3′ (E386S), 5′-GCAGATTGAACGCGAGCACAAC-GGGTACATGGAG-3′ (L389H), 5′-CGAGCTCAACGGGTCCATGGAGTGG-ATCTCAAAAGC-3′ (Y392S) and 5′-GGATCTCAAAAGCAGCTGA-GGTGATCCTCGCAGAGG-3′ (E400A). The selection primer 5′-GACATCC-CTTGGATATCATCGTGACTG-3′ was used to mutate *Eco*RI to *Eco*RV on the recombinant PGEX2T molecule. All mutations were verified by sequence analysis. Overlays were done as described in Fig. 1 legend. Autoradiographs were scanned with a Molecular Dynamics computing densitometer.

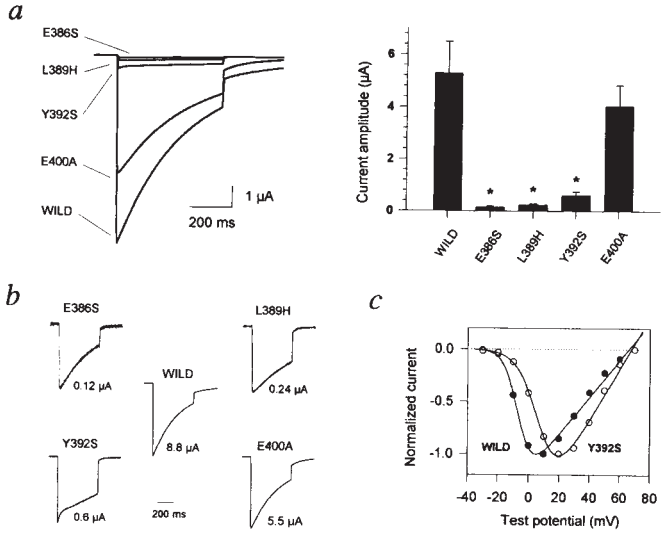


FIG. 4 Mutagenesis of the $\beta$-subunit interaction site on the $\alpha_{1A}$ subunit alters the effects of $\alpha_1$–$\beta$ subunit coexpression. *a*, Barium currents of $\alpha_{1A}$ (WILD) or mutated $\alpha_{1A}$-subunits (E386S, L389H, Y392S and E400A) coexpressed with $\alpha_{2b}$- and $\beta_{1b}$-subunits in *Xenopus* oocytes. Left panel shows superimposed representative traces of $Ba^{2+}$ currents evoked from a holding potential of −90 mV to a +10 mV test potential (TP). Right panel shows average peak currents obtained ($n = 7$ to 9 oocytes). Statistically significant reductions ($P < 0.05$, *t*-test) from wild-type $\alpha_{1A}$ expression levels are denoted by asterisks. Error bars are s.e.m. *b*, Same representative current traces as in *a*, illustrating changes in inactivation kinetics. *c*, Normalized average current–voltage relationship from $\alpha_{1A}$ (WILD) or mutated $\alpha_{1A}$-subunit (Y392S) to show shift in peak currents induced by the Y392S point mutation. Smooth curves were generated assuming an activation curve of a Boltzmann type $I_{Ba} = [g(TP-E)]/[1 + \exp(-(TP-V_{1/2})/k)]$ with $g$, the maximum normalized conductance ($g_{WILD} = 0.018$ and $g_{Y392S} = 0.024$), $E$, the reversal potential ($E_{WILD} = 66$ mV and $E_{Y392S} = 68$ mV), and $V_{1/2}$, the potential of half-activation ($V_{1/2,WILD} = -6.4$ mV and $V_{1/2,Y392S} = 7.6$ mV) and $k$, the range of potential for an e-fold change around $V_{1/2}$ ($k_{WILD} = 4.6$ mV and $k_{Y392S} = 6.7$ mV).

METHODS. To mutate the full-length $\alpha_{1A}$-subunit, pSPCBI-2 (ref. 12), base pairs 1,282–1,745 were amplified by PCR and subcloned into a T-vector made from Bluescript SK$^-$. Mutagenic primers and a selection primer, 5′-CATGGTCAATCATGCTTATCGATAC-3′, which eliminates the *Hin*dIII site on the recombinant molecule, were used. The 1,416–1,723 *Bsm*I fragment encoding the motif in $\alpha_{1A}$ was then replaced with mutated *Bsm*I fragments from the T-vector constructs. To facilitate cloning, the third *Bsm*I site in the 3′ non-coding region was deleted by digestion at two flanking *Bam*HI sites, followed by recircularization of the plasmid. This *Bam*HI fragment was restored after subcloning the mutated *Bsm*I fragments. The mutated regions were sequenced in both directions on an Applied Biosystems Inc. Automated Sequencer. Complementary RNAs were transcribed *in vitro* using SP6 RNA polymerase with the rabbit brain $\alpha_{1A}$ plasmid or $\alpha_{1A}$ mutants E386S, L389H, Y392S and E400A, and T7 RNA polymerase with rat brain $\alpha_{2b}$ and $\beta_{1b}$ plasmids. Wild-type or mutant $\alpha_{1A}$-subunits were co-injected with $\alpha_{2b}$ and $\beta_{1b}$ into stage V or VI *Xenopus* oocytes at concentrations: 0.6 μg ml$^{-1}$ $\alpha_{1A}$ or mutants, 0.4 μg ml$^{-1}$ $\alpha_{2b}$ and 0.2 μg ml$^{-1}$ $\beta_{1b}$; about 50 nl was injected per cell. $Ba^{2+}$ currents were recorded by a standard two-microelectrode voltage-clamp using a Dagan amplifier (TEV-200). Voltage and current electrodes (0.5–2 MΩ tip resistance) were filled with 3 M KCl. The bath solution was (in mM): $Ba(OH)_2$, 40; NaOH, 50; KCl, 2; niflumic acid, 1; EGTA, 0.1; HEPES, 5; pH 7.4, adjusted with methanesulphonic acid. Records were filtered at 0.2 to 0.5 kHz and sampled at 1–2 kHz. Leak and capacitance currents were subtracted off-line by a P/4 protocol. $Ba^{2+}$ current through endogenous channels was less than 10 nA (no injection) and average $Ba^{2+}$ current was 40 nA upon injection of $\beta_{1b}$ and $\alpha_{2b}$ cRNAs.

the $\beta$-subunit was determined by the overlay assay described above. The $\beta$-subunit interaction was reduced with the $E386S_{FP}$, $L389H_{FP}$ and $Y392S_{FP}$ mutants compared with the wild-type epitope (Fig. 3*a*, *b*). This reduction was greatest with the $Y392S_{FP}$ mutation, which required prolonged exposure of the film for visualization. No reduction in intensity was observed with $E400A_{FP}$. Densitometric scans of autoradiogram band intensities normalized for protein concentration and averaged over three experiments measured a 27-fold reduction in $\beta$-subunit binding to $Y392S_{FP}$ compared with the wild-type epitope. Binding to mutants $E386S_{FP}$ and $L389H_{FP}$ were both reduced 1.7-fold, whereas a 1.3-fold enhancement was measured with $E400A_{FP}$.

Coexpression of $\alpha_{1A}$ with a $\beta$-subunit dramatically increases the functional expression[12] and alters the voltage-dependent and kinetic properties of the channel in *Xenopus* oocytes (not shown). Alteration of the $\beta$-subunit binding motif on $\alpha_{1A}$ should therefore alter the modulatory contribution by the $\beta$-subunit. A deletion of 30 amino acids that includes the interaction motif ($\alpha_{1A}$377–406) or a smaller 16-amino-acid deletion ($\alpha_{1A}$377–393) of part of the motif had the result that no detectable current (<10 nA) was observed on coexpression with the $\beta_{1b}$-subunit in *Xenopus* oocytes (not shown). To determine more accurately the functional importance of the motif, the four point mutations described above were introduced into the full-length $\alpha_{1A}$-subunit. Coexpression of $E386S_{\alpha 1A}$, $L389H_{\alpha 1A}$ or $Y392S_{\alpha 1A}$ with $\alpha_{2b}$- and $\beta_{1b}$-subunits resulted in significantly reduced peak currents compared with the wild-type $\alpha_{1A}$-subunit (Fig. 4*a*). Average reductions in current expression were: $E386S_{\alpha 1A}$, 36-fold; $L389H_{\alpha 1A}$, 22-fold; $Y392S_{\alpha 1A}$, 9-fold; $E400A_{\alpha 1A}$, 1.3-fold. Although autoradiogram band intensities of $\beta$-subunit overlay were also reduced for mutations E386S, L389H and Y392S, no quantitative correlations were attempted because of the vastly different conditions of these assays. Mutant $Y392S_{\alpha 1A}$ altered the inactivation kinetics of the channel (Fig. 4*b*). At test pulses to +10 mV, $Ba^{2+}$ current inactivated with similar average time constants of (mean ± s.d.) $\tau = 350 \pm 59$ ms (wild-type $\alpha_{1A}$, $n = 7$), $\tau = 290 \pm 69$ ms ($E386S_{\alpha 1A}$, $n = 9$), $\tau = 434 \pm 158$ ms ($L389H_{\alpha 1A}$, $n = 8$) and $\tau = 522 \pm 119$ ms ($E400A_{\alpha 1A}$, $n = 7$). However, $Ba^{2+}$ current conducted by $Y392S_{\alpha 1A}$ consistently inactivated along two components, $\tau_1 = 22 \pm 4$ ms (15% of the total current) and $\tau_2 = 1{,}806 \pm 682$ ms (85% of the total current). In addition to this change in inactivation kinetics, this Y392S mutation also shifted the voltage-dependence of activation (Fig. 4*c*). All currents, independent of magnitude, peaked at a test potential of +10 mV, except for $Y392S_{\alpha 1A}$, which peaked at +20 mV. More precise estimates of $Y392S_{\alpha 1A}$ peak currents were obtained by a fit of the data and showed a general shift by 15 mV towards depolarized test potentials. Although the Y392S mutation greatly modified the biophysical properties of $\alpha_{1A}\alpha_{2b}\beta_{1b}$ complexes, this was not due to a complete loss of $\alpha_1$–$\beta$-subunit interaction. $\beta_{1b}$-subunit still overlayed on the mutant epitope (Fig. 3*b*) and also, peak current amplitudes with $Y392S_{\alpha 1A}\alpha_{2b}$ were enhanced from (mean ± s.e.m.) $-10 \pm 4$ nA ($n = 4$) to $-613 \pm 137$ nA ($n = 8$) by $\beta_{1b}$-subunit coexpression. $Ba^{2+}$ currents obtained in the absence of the $\beta_{1b}$-subunit were, however, too small for accurate description of the current properties.

The non-conserved residues interspersed among conserved amino acids of the $\beta$-subunit interaction motif may be important for the variation in effects of $\beta$-subunits on different $\alpha_1$-subunits. For example, when the $\alpha_{1E}$-subunit is coexpressed with the $\beta$-subunit, shifts in voltage-dependence of activation and inactivation occur, but no appreciable stimulation of current expression is observed[9]. Sequence variations of the motif in the carp skeletal muscle $\alpha_1$-subunit[21] in position 4 (E→D) and in an $\alpha_1$ subunit (doe-4)[22] of torpedo electric organ at positions 7 (L→F) and 9 (G→R) may indicate differences in modulation by $\beta$-subunits in these non-mammalian channels or a structural divergence in their respective $\beta$-subunits to accommodate these substitutions. Our results show that substitutions of critical residues in the $\beta$-subunit interaction motif on the $Ca^{2+}$ channel $\alpha_1$-subunit alter the ability of the $\alpha_1$-subunit to be modulated by the $\beta$-subunit. The properties altered by these mutations correlate well with those modified by $\beta$-subunits on coexpression with $\alpha_1$-subunits[4 12]. These findings suggest a critical role for the conserved interaction site on the I–II cytoplasmic linker of the $\alpha_1$-subunit in voltage-sensitive calcium-channel modulation by the $\beta$-subunit. □

Received 1 November; accepted 21 December 1993.


1. Catterall, W. A., Seagar, M. J. & Takahashi, M. *J. biol. Chem.* **263,** 3535–3538 (1987).
2. Campbell, K. P., Leung, A. T. & Sharp, A. H. *Trends Neurosci.* **11,** 425–430 (1988).
3. Witcher, D. R. *et al. Science* **261,** 486–489 (1993).
4. Lacerda, A. E. *et al. Nature* **352,** 527–530 (1991).
5. Perez-Reyes, E. *et al. J. biol. Chem.* **267,** 1792–1797 (1992).
6. Williams, M. E. *et al. Neuron* **8,** 71–84 (1992).
7. Castellano, A., Wei, X., Birnbaumer, L. & Perez-Reyes, E. *J. biol. Chem.* **268,** 3450–3455 (1993).
8. Castellano, A., Wei, X., Birnbaumer, L. & Perez-Reyes, E. *J. biol. Chem.* **268,** 12359–12366 (1993).
9. Soong, T.-W. *et al. Science* **260,** 1133–1136 (1993).
10. Stea, A. *et al. Neuropharmacology* **32,** 1103–1116 (1993).
11. Nishimura, S., Takeshima, H., Hofmann, F., Flockerzi, V. & Imoto, K. *FEBS Lett.* **324,** 283–286 (1993).
12. Mori, Y. *et al. Nature* **350,** 398–402 (1991).
13. Neely, A., Wei, X., Olcese, R., Birnbaumer, L. & Stefani, E. *Science* **262,** 575–578 (1993).
14. Pragnell, M., Sakamoto, J., Jay, S. D. & Campbell, K. P. *FEBS Lett.* **291,** 253–258 (1991).
15. Leung, A. T., Imagawa, T. & Campbell, K. P. *J. biol. Chem.* **262,** 7943–7946 (1987).
16. Ellis, S. B. *et al. Science* **241,** 1661–1664 (1988).
17. Dubel, S. J. *et al. Proc. natn. Acad. Sci. U.S.A.* **89,** 5058–5062 (1992).
18. Altschul, S. F., Gish, W., Miller, W., Myers, E. W. & Lipman, D. *J. molec. Biol.* **215,** 403–410 (1990).
19. Biel, M. *et al. FEBS Lett.* **269,** 409–412 (1990).
20. Hui, A. *et al. Neuron* **7,** 35–44 (1991).
21. Grabner, M. *et al. Proc. natn. Acad. Sci. U.S.A.* **88,** 727–731 (1991).
22. Horne, W. A. *et al. Proc. natn. Acad. Sci. U.S.A.* **90,** 3787–3791 (1993).
23. Marchuk, D., Drumm, M., Saulino, A. & Collins, S. F. *Nucleic Acids Res.* **19,** 1154 (1991).


ACKNOWLEDGEMENTS. We thank L. Birnbaumer and X. Wei for the $\alpha_{1C\text{-}a}$ subunit cDNA; S. D. Kahl and W. Guo for technical assistance; and B. A. Adams, T. Hoshi, S. L. Roberds, E. Shibata, A. Stea and D. R. Witcher for comments on the manuscript. K.P.C. and T.T. are investigators of HHMI; T.P.S. is an HHMI International Research Scholar and is also supported by a grant from the MRC of Canada.

# A 13-amino-acid motif in the cytoplasmic domain of FcγRIIB modulates B-cell receptor signalling

**Tatsushi Muta*, Tomohiro Kurosaki†, Ziva Misulovin‡, Mercedes Sanchez‡, Michel C. Nussenzweig‡ & Jeffrey V. Ravetch***

* DeWitt Wallace Research Laboratory, Sloan–Kettering Institute, 1275 York Avenue, New York, New York 10021, USA
‡ The Rockefeller University, 1230 York Avenue, New York, New York 10021, USA

**THE Fc receptor on B lymphocytes, FcγRIIB (β1 isoform), helps to modulate B-cell activation triggered by the surface immunoglobulin complex[1,2]. Crosslinking of membrane immunoglobulin by antigen or anti-Ig $F(ab')_2$ antibody induces a transient increase in cytosolic free $Ca^{2+}$, a rise in inositol-3-phosphate, activation of protein kinase C, and enhanced protein tyrosine phosphorylation[3–5]. Crosslinking FcγRIIB with the surface immunoglobulin complex confers a dominant signal that prevents or aborts lymphocyte activation triggered through the ARH-1 motifs of the signal transduction subunits Ig-α and Ig-β. Here we show that FcγRIIB modulates membrane immunoglobulin-induced $Ca^{2+}$ mobilization by inhibiting $Ca^{2+}$ influx, without changing the pattern of tyrosine phosphorylation. A 13-amino-acid motif in the cytoplasmic domain of FcγRIIB is both necessary and sufficient for this effect. Tyrosine**

† Department of Cardiovascular Molecular Biology, Lederle Laboratories, 401 North Middletown Road, Pearl River, New York 10965, USA.